Hot oxygen atoms in the Venus nightside exosphere

H. Gröller, H. Lammer, H. I. M. Lichtenegger, M. Pfleger, O. Dutuit, V. I. Shematovich, Y. N. Kulikov, H. K. Biernat

Hot oxygen atoms in the Venus nightside exosphere

H. Gröller,[1] H. Lammer,[1] H. I. M. Lichtenegger,[1] M. Pfleger,[2] O. Dutuit,[1,3] V. I. Shematovich,[4] Y. N. Kulikov,[5] and H. K. Biernat[1,2]

Received 24 November 2011; revised 11 January 2012; accepted 12 January 2012; published 10 February 2012.

[1] The nightside oxygen exosphere of Venus is investigated for high and moderate solar activity by means of a Monte-Carlo model. Hot O atoms are assumed to be produced by dissociative recombination of O_2^+ and NO^+ molecular ions and by charge transfer processes between ionospheric O^+ ions and neutral O and H atoms. The model considers rotational and vibrational excitation of the initial energy distribution of hot O atoms, includes elastic, inelastic, and quenching collisions between the suprathermal atoms and the ambient neutral atmosphere species, and uses differential cross sections for the determination of the scattering angle in the collisions. The results indicate that dissociative recombination of O_2^+ is, like at Venus' dayside, the most efficient source of hot O atoms at the planet's nightside. For high solar activity, the nightside exospheric density of hot O atoms is about one order of magnitude lower compared to the dayside, although between 2–10 times higher than in previous studies. **Citation:** Gröller, H., H. Lammer, H. I. M. Lichtenegger, M. Pfleger, O. Dutuit, V. I. Shematovich, Y. N. Kulikov, and H. K. Biernat (2012), Hot oxygen atoms in the Venus nightside exosphere, *Geophys. Res. Lett.*, *39*, L03202, doi:10.1029/2011GL050421.

1. Introduction

[2] Numerical modeling of the stochastic motion of hot atoms produced in exothermic processes in the thermosphere of Venus suggests that the dayside exosphere of the planet is dominated by a hot O atom corona [e.g., *Nagy et al.*, 1981; *Nagy and Cravens*, 1988; *Ip*, 1988; *Kim et al.*, 1998; *Hodges*, 2000; *Krestyanikova and Shematovich*, 2006; *Lammer et al.*, 2006; *Lichtenegger et al.*, 2009; *Valeille et al.*, 2010; *Gröller et al.*, 2010]. The observational evidence of such a corona is based on the interpretation of data obtained by the UV spectrometers aboard Pioneer Venus Orbiter (PVO) [*Nagy et al.*, 1981; *Nagy and Cravens*, 1988] and Venera 11 [*Bertaux et al.*, 1981] three decades ago. However, these early observations have not been confirmed so far by ESA's Venus Express mission with the UV and IR spectrometers (SPICAV). Recently *Gröller et al.* [2010] applied an advanced Monte-Carlo model which determines the initial velocity distribution of hot oxygen atoms – which are produced via dissociative recombination of O_2^+ ions – by means of an energy dependent rate coefficient and by taking into account the vibrational and rotational energies of the nascent hot atoms. In this model, the motion of the suprathermal particles is simulated by considering elastic, inelastic, and quenching collisions, thereby using energy and mass dependent total collision cross sections and their corresponding differential cross sections which allow the calculation of the scattering angle and the energy transfer in a collision. *Gröller et al.* [2010] found that the hot O dayside densities inferred from the PVO observations during high solar activity could only be reproduced on the basis of a forward scattering model but disregarding inelastic and quenching collisions. This discrepancy between our simulations and the *Nagy et al.* [1981] observations, which are based on a single data set may be due to special measurement conditions; indeed Venera 12 could not confirm these data 4 days later [*Bertaux et al.*, 1981].

[3] The nightside ionosphere of Venus is not only highly variable in time and space [*Spenner et al.*, 1995], it is also strongly influenced by ion transport processes from the dayside and one may therefore expect a highly fluctuating nightside exosphere. The aim of this study is to investigate the nightside exosphere of Venus, which is not well studied so far, by applying the model of *Gröller et al.* [2010] in order to better understand the role of the nightside production of the hot O atoms and its contribution to the exosphere structure and behavior. In section 2 we discuss the available ion and neutral atmosphere input parameters. Section 3 describes various processes which can produce a hot O population on the nightside. Section 4 focusses on the energy distribution functions of hot O atoms which are obtained by accounting for the energy loss of the hot particles in collisions with the cold background atmosphere when moving through the nightside upper atmosphere. Finally, the hot O corona density at the nightside is presented and compared with the corresponding dayside densities as well as with the results obtained by *Nagy et al.* [1981] and *Hodges* [2000].

2. Nightside Atmosphere and Ionosphere

[4] Since neither neutral or ion densities nor temperature profiles of the nightside are available from the current Venus Express (VEX) Mission, modeled profiles for the nightside of Venus based on the PVO observations are used in the simulations. The orbiter retarding potential analyzer (ORPA) on board of PVO measured the major ion composition, including density and temperature, over a time span of 14 years. From these observations it was found that Venus' nightside ionosphere densities vary highly during the solar cycle. At high solar activity (HSA) the nightside ion density can be surprisingly high [*Spenner et al.*, 1995] with O_2^+ ion

[1]Space Research Institute, Austrian Academy of Sciences, Graz, Austria.
[2]Institute of Physics, University of Graz, Graz, Austria.
[3]Institut de Planétologie et d'Astrophysique de Grenoble, CNRS-UJF, Grenoble, France.
[4]Institute of Astronomy, Russian Academy of Sciences, Moscow, Russia.
[5]Polar Geophysical Institute, Russian Academy of Sciences, Murmansk, Russia.

0094-8276/12/2011GL050421

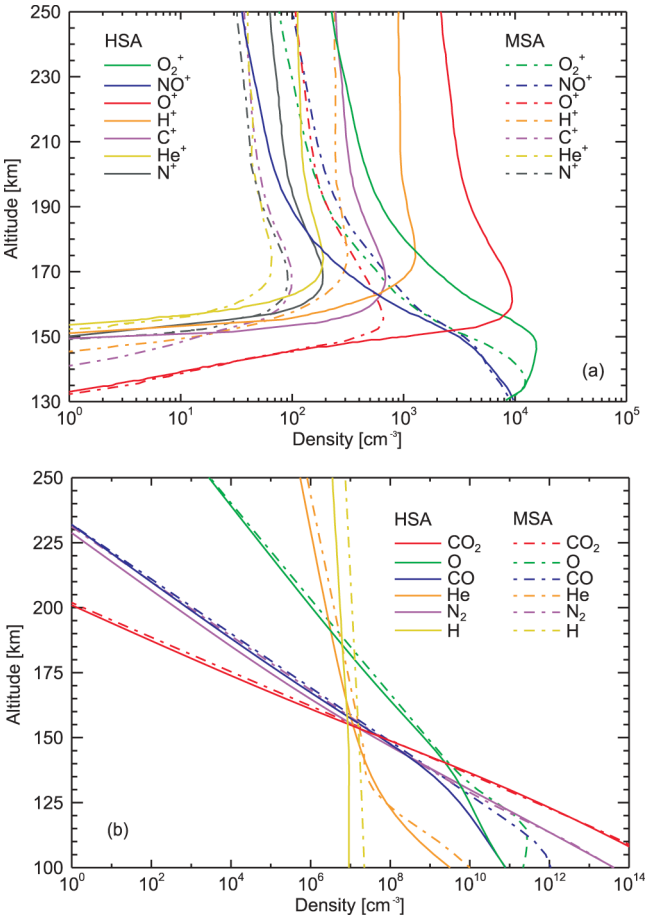

Figure 1. Altitude dependent (a) ion and (b) neutral density profiles for high (solid lines) and moderate (dashed-dotted lines) solar activity conditions [*Dobe et al.*, 1995; *Hedin et al.*, 1983; *Brannon and Fox*, 1994; *Keating et al.*, 1985].

number densities of more than 10^4 cm^{-3} (from ~150 up to ~250 km), while during moderate solar activity (MSA), especially in the upper nightside ionosphere, the density could be strongly depleted [*Knudsen et al.*, 1987]. PVO/OPRA observations of fast moving O^+ ions from the Venus dayside across the terminator indicate that transport processes related to the solar activity play a large role in the formation and modification of the nightside ionosphere of Venus [*Knudsen et al.*, 1980, 1987; *Kliore et al.*, 1991].

[5] Because PVO was far above the Venus nightside ionopause during the 1985 solar minimum, there exist no observational data for low solar activity (LSA). Therefore we restrict our present study to high and moderate solar activity conditions and adopt the modeled ion density profiles for HSA ($F_{10.7}$ = 200) and MSA ($F_{10.7}$ = 120–150) from Figures 3 and 7, respectively, of *Dobe et al.* [1995]; they are displayed in Figure 1a. The neutral density profiles for midnight at the equator and HSA are taken from Table 3a of *Hedin et al.* [1983] and from Figure 1a of *Brannon and Fox* [1994], based on *Brinton et al.* [1980]. For MSA ($F_{10.7}$ = 150) the data given in Table 4–5 (for 150–250 km altitude) and Table 4–14 (for 100–150 km altitude) from *Keating et al.* [1985] are used. Figure 1b illustrates the neutral density profiles for high and moderate solar activity used as input in our simulations. The ion and electron temperatures (T_i and T_e) for HSA are taken from Figures 2 and 3 of *Miller et al.* [1980], while for MSA T_i is obtained from Figure 3 of *Spenner et al.* [1995] and T_e from Figure 3b of *Theis and Brace* [1993]. It should be noted that T_i and T_e for HSA and T_i for MSA are valid for a solar zenith angle between 150°–180° and that both temperatures for MSA correspond to a solar flux of $F_{10.7}$ = 120 and are given only down to an altitude of about 150 km. Since at altitudes <150 km T_i and T_e are comparable to the neutral temperature T_n, we assume $T_i = T_e = T_n$ down to 100 km.

3. Hot O Atom Production

3.1. Sources of Hot Atoms

[6] In addition to dissociative recombination (DR) of O_2^+ ions [e.g., *Nagy et al.*, 1981; *Krestyanikova and Shematovich*, 2005, 2006; *Lichtenegger et al.*, 2009; *Gröller et al.*, 2010], the following reactions are assumed to produce suprathermal oxygen atoms in the nightside of Venus: DR of NO^+ ions, charge transfer (CT) of O^+ ions with ambient O, CO_2, and H, and radiative recombination of $O^+ + e$.

3.1.1. Dissociative Recombination

[7] As shown by *Gröller et al.* [2010], higher vibrational levels for O_2^+ ions have a minor effect on the energy distribution functions of the dayside and we expect a similar behavior for the nightside; therefore only the vibrational ground state is taken into account for the O_2^+ ions.

[8] The dissociative recombination of NO^+ proceeds via the following channels

$$NO^+ + e \rightarrow \begin{cases} N(^4S) + O(^3P) + 2.77 \text{ eV}[0.15] \\ N(^4S) + O(^1D) + 0.80 \text{ eV}[0.00] \\ N(^2D) + O(^3P) + 0.38 \text{ eV}[0.85] \end{cases}. \quad (1)$$

The given excess energies are valid for the vibrational ground state of the $NO^+(X^1\Sigma^+)$ ions. The radiative lifetimes of 90, 49, 30, 25, and 19 ms for vibrationally excited (v = 1, 2, 3, 4, 5) $NO^+(X^1\Sigma^+)$ measured by *Wyttenbach et al.* [1991] are short compared to the typical time between collisions at the considered altitudes, therefore the vibrational excited states can be neglected. The branching ratio, given in squared brackets in (1), are taken from *Vejby-Christensen et al.* [1998] and *Sheehan and St.-Maurice* [2004] and valid for a very low relative collision energy. Due to the lack of other data, we assume that these values also apply to higher collision energies. The production rate for DR of NO^+ ions is calculated using the electron temperature dependent rate coefficient α, given by

$$\alpha = A_f \left(\frac{T_e}{300}\right)^{\beta} \text{ cm}^3 \text{ s}^{-1} \quad (2)$$

according to *Sheehan and St.-Maurice* [2004], with the coefficients $A_f = 3.50 \times 10^{-7}$ and $\beta = -0.69$ for $T_e < 1200$ K and $A_f = 3.02 \times 10^{-7}$ and $\beta = -0.56$ for $T_e > 1200$ K for the electronic and vibrational ground state.

[9] The rotational energy for the $^1\Sigma$ state, the simplest molecular state, is obtained from the rotational term $F_v(J)$ with [*Herzberg*, 1950]

$$F_v(J) = B_v J(J+1) - D_v J^2 (J+1)^2, \quad (3)$$

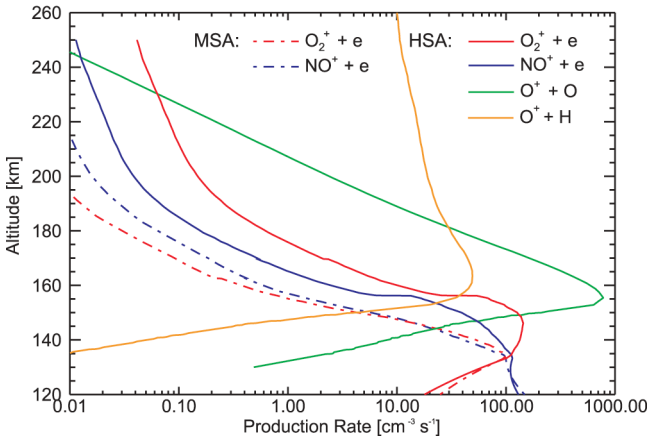

Figure 2. Altitude dependent hot O atom production rates from the dissociative recombination of O_2^+ and NO^+, as well as for the charge transfer between O^+ and O and H. The solid and the dashed-dotted lines are for high and moderate solar activity, respectively.

where the rotation constant B_v reads

$$B_v = B_e - \alpha_e\left(v+\frac{1}{2}\right) + \gamma_e\left(v+\frac{1}{2}\right)^2 + \delta_e\left(v+\frac{1}{2}\right)^3 \quad (4)$$

and the centrifugal distortion constant D_v reads

$$D_v = D_e + \beta_e\left(v+\frac{1}{2}\right). \quad (5)$$

The value for the equilibrium internuclear distance B_e = 1.99727 cm^{-1}, as well as those for the coefficients α_e = 0.01889 cm^{-1}, $\gamma_e = \delta_e = 0\ cm^{-1}$, $D_e = 5.64 \times 10^{-6}\ cm^{-1}$, and $\beta_e = 0\ cm^{-1}$ are taken from *Huber and Herzberg* [2011].

3.1.2. Charge Transfer

[10] Charge transfer of O^+ with the main background constituents O, H, and CO_2 yields hot $O(^3P)$ atoms according to

$$O^+(^4S) + O \rightarrow O(^3P) + O^+, \quad (6)$$

$$O^+(^4S) + H \rightarrow O(^3P) + H^+, \quad (7)$$

$$O^+(^4S) + CO_2 \rightarrow \begin{cases} O(^3P) + CO_2^+ - 0.16\ \text{eV} \\ O_2^+ + CO + 1.2\ \text{eV}. \end{cases} \quad (8)$$

The production rates of $O(^3P)$ atoms for reaction (6) is calculated by using a rate coefficient equal to $1.6 \times 10^{-11}(T_n + T_i)^{0.5}$ $cm^3\ s^{-1}$ taken from *Terada et al.* [2002]. The rate coefficient for CT with H is taken from the UDFA06 database [*Woodall et al.*, 2007] based on *Stancil et al.* [1999] as

$$\alpha = A_f\left(\frac{T}{300}\right)^{\beta} \exp\frac{-\gamma}{T}\ \ cm^3\ s^{-1} \quad (9)$$

with the gas temperature T and the coefficients $A_f = 5.66 \times 10^{-10}$, $\beta = 0.36$, and $\gamma = -8.6$ for a two-body reaction.

[11] The reaction (8) has two channels in the interesting energy range, one slightly endothermic channel producing O atoms and one exothermic channel producing O_2^+, with a total rate coefficient of 5×10^{-10} $cm^3\ s^{-1}$ [*Alcaraz et al.*, 2004]. In the considered altitude range most of the newly produced hot O atoms gain energies less than 0.2 eV with branching ratios lower than 20% [*Alcaraz et al.*, 2004] and therefore this reaction is neglected.

3.1.3. Radiative Recombination

[12] The radiative recombination corresponding to

$$O^+ + e \rightarrow O + h\nu \quad (10)$$

results only in very low production rates with a maximum of $\sim 10^{-3}$ $cm^{-3}\ s^{-1}$ at about 160 km altitude (calculated by means of equation (9) with $A_f = 3.24 \times 10^{-12}$, $\beta = -0.66$, and $\gamma = 0$ taken from the UDFA06 database [*Woodall et al.*, 2007] based on *Nahar* [1999]). Hence this additional source is also neglected in the simulations.

3.2. Production Rate

[13] The altitude dependent production rates for DR of O_2^+ and NO^+, as well as for CT between O^+ and O and H, are shown in Figure 2, where the solid and the dashed-dotted lines correspond to HSA and MSA, respectively. Although the CT rate coefficient between O^+ and O is very small compared to the DR coefficients of O_2^+ and NO^+, the production rate is up to one order of magnitude higher because of the high neutral O density.

3.3. Neutral Collisions

[14] Collisions between the traced hot O atoms and the ambient cool constituents O, CO_2, CO, N_2, H, and He are included in the model. The total and differential cross sections for O-H collisions are taken from *Zhang et al.* [2009], where the former is given in the energy range from 0–10 eV and the differential cross sections are given for scattering energies of 0.1, 1.0, 5.0, and 10.0 eV. For other collision energies the corresponding nearest energy is used. The same set of collision cross sections is also taken for the collisions between the hot O atoms and the ambient He particles.

4. Nightside Exosphere

[15] Based on the ion and neutral atmosphere density profiles shown in Figure 1 and on the hot O atom production rates given in Figure 2, the Monte-Carlo model of *Gröller et al.* [2010] is applied to calculate the energy distribution functions (EDFs) at the exobase level of about 160 km altitude for nightside conditions.

[16] Figure 3a shows the EDFs for hot O atoms originating from DR of O_2^+ and NO^+, as well as from CT of O^+ with O and H for high solar activity, as the sum of the hot and cool background O population. The grey solid and dashed-dotted lines represent the Maxwell distribution of the oxygen background for the high and moderate solar activity levels, respectively. In addition, for MSA only the EDFs of O resulting from DR of O_2^+ and NO^+ are displayed, because they are – similar to the HSA case – the most important sources.

[17] In Figure 3b the total EDFs (i.e., the sum of all sources of hot O atoms) for HSA (red) and MSA (green) at 160 km are illustrated. Additionally, the simulated nightside EDF at 143 km exobase altitude from *Nagy et al.* [1981] (black) is shown. It should be noted that this exobase level is ~17 km

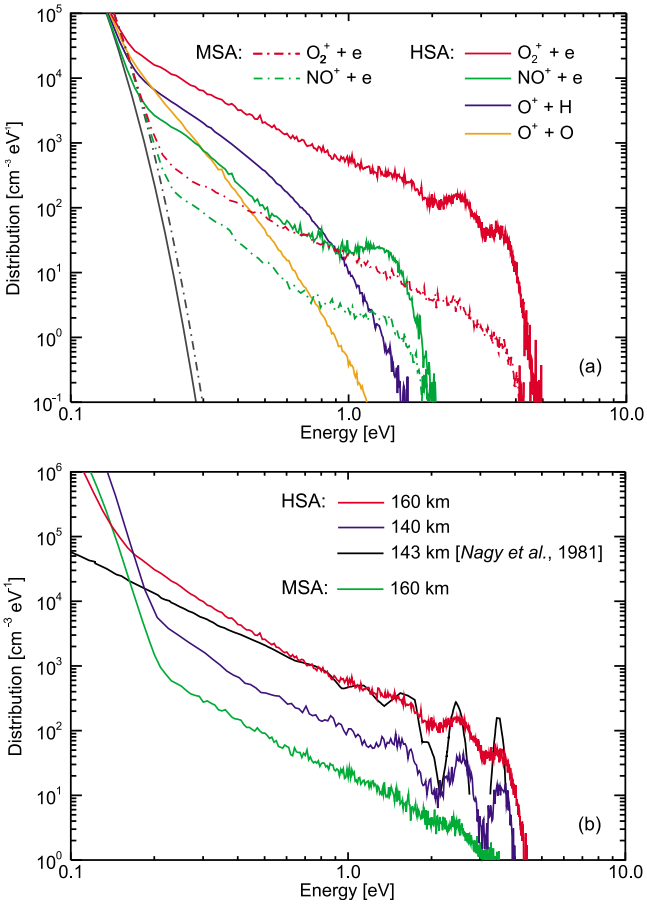

Figure 3. (a) Energy distribution functions (EDFs) at an altitude of 160 km for the dissociative recombination of O_2^+ and NO^+, as well as the charge transfer of O^+ with O and H for the high and the first two reactions for the moderate solar activity case. The gray solid and dashed-dotted lines represent the Maxwell distribution of the oxygen background for high and moderate solar activity, respectively. (b) The total EDFs for high and moderate solar activity at 160 km. Additionally, in Figure 3b the simulated nightside EDF at 143 km altitude from *Nagy et al.* [1981] is given. For comparison reason also the EDF at 140 km for high solar activity is shown.

lower than the one (160 km) calculated by our model; the exobase is located where the mean free path of O atoms equals the scale height [*Gröller et al.*, 2010]. For comparison also the 140 km altitude EDF of our simulation is displayed.

[18] Upon assuming that there are no collisions above the exobase, the EDFs of Figure 3, together with the direction of the upward velocities – determined as well by the Monte-Carlo model – can be used to calculate the initial velocities for the particles populating the exosphere and moving along Keplerian orbits. Figure 4a displays the exosphere density of hot oxygen atoms for high (solid) and moderate (dashed-dotted) solar activity separated by the various reactions.

[19] Although the O_2^+ and NO^+ densities are quite similar during MSA (Figure 1a), the contribution of the DR of NO^+ to the O density is about one order of magnitude lower than those produced by DR of O_2^+. This is due to the higher initial energies of up to 6 eV gained by DR of O_2^+ with respect to a maximum of 2.5 eV attained by DR of NO^+. Further, despite the relatively high production rates of the CT reactions (6) and (7), the density of hot O originating from these sources significantly decreases with altitude due to their low initial energies. Therefore, we conclude that the main contribution to the nightside hot O corona of Venus is – as on the dayside – due to the DR of O_2^+.

[20] In Figure 4b the total nightside hot O density profiles for HSA (red) and MSA (green) based on the EDFs at 160 km are shown together with the corresponding densities from *Nagy et al.* [1981] (black) and *Hodges* [2000] (gray). For comparison with the density profile of *Nagy et al.* [1981] also the profile (blue) based on the 140 km altitude EDF is drawn. The density obtained from the EDFs at 160 km altitude, which represents our calculated exobase altitude, is about a factor of two higher than the profile of *Nagy et al.* [1981] (which is based on a 143 km exobase level, however). Moreover, for altitudes above 300 km, our density is between a factor of 6 and 10 higher than the one published by *Hodges* [2000] who assumed an exobase altitude of 150 km. One of

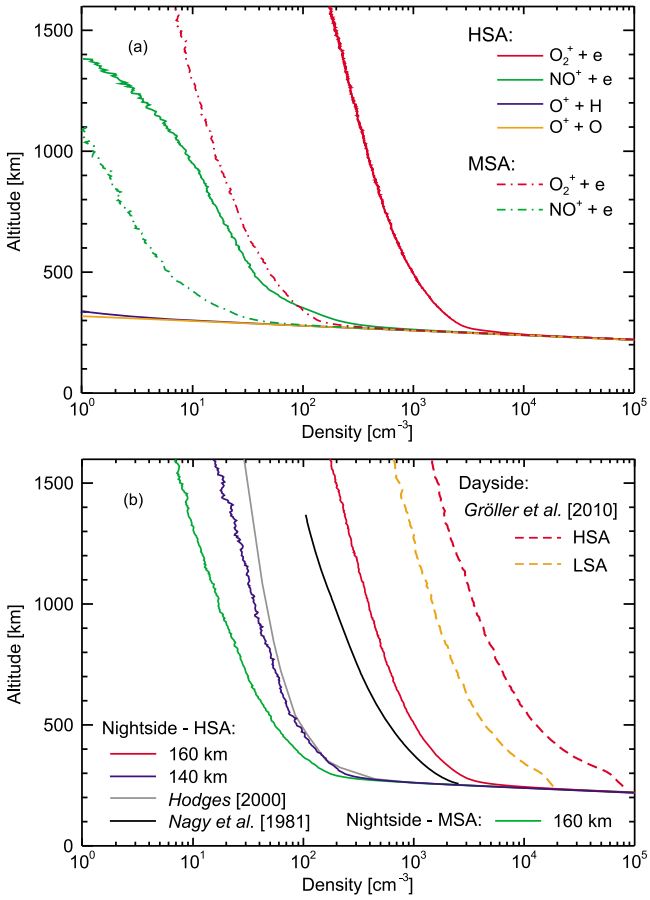

Figure 4. (a) Altitude dependent hot oxygen densities for the dissociative recombination of O_2^+ and NO^+ for high and moderate, as well as the charge transfer of O^+ with O and H for the high solar activity case. (b) The densities for high and moderate solar activity using the EDFs at 160 km. Additionally, in Figure 4b the simulated nightside hot oxygen density from *Nagy et al.* [1981], using the EDF at 143 km altitude, and from *Hodges* [2000] are given. For comparison reason the EDF at 140 km for high solar activity and also the dayside density profiles from *Gröller et al.* [2010] are shown.

the main reason for these differences is our use of energy dependent cross sections in contrast to a constant one assumed by the above authors.

[21] Finally, we note that the hot O atom density for HSA at Venus nightside is about one order of magnitude lower than the density at the dayside [*Gröller et al.*, 2010].

5. Conclusions

[22] By studying a number of possible sources for hot oxygen atoms and applying a Monte-Carlo model to simulate the stochastic motion of these particles, we found that similar to the dayside, dissociative recombination of O_2^+ is the main source of hot O atoms on the nightside. For high solar activity, the nightside oxygen exobase is predicted at ∼160 km altitude and the exosphere O density appears to be about one order of magnitude lower compared to the dayside.

[23] **Acknowledgments.** This research has been supported by the Helmholtz Association through the research alliance "Planetary Evolution and Life" and through the joined Russian-Austrian project under the RFBR grant 09-02-91002-215-ANF-a and the FWF grant I199-N16. V. I. S. is supported by the RFBR grant 11-02-00479. H. G. thanks Michel Vervloet for very helpful discussions.

[24] The Editor thanks an anonymous reviewer for his or her assistance in evaluating this paper.

References

Alcaraz, C., C. Nicolas, R. Thissen, J. Zabka, and O. Dutuit (2004), $^{15}N^+ + CD_4$ and $O^+ + {}^{13}CO_2$ state-selected ion-molecule reactions relevant to the chemistry of planetary ionospheres, *J. Phys. Chem. A*, *108*(45), 9998–10,009, doi:10.1021/jp0477755.

Bertaux, J., J. E. Blamont, V. M. Lepine, V. G. Kurt, N. N. Romanova, and A. S. Smirnov (1981), Venera 11 and Venera 12 observations of E.U.V. emissions from the upper atmosphere of Venus, *Planet. Space Sci.*, *29*(2), 149–166, doi:10.1016/0032-0633(81)90029-5.

Brannon, J. F., and J. L. Fox (1994), The downward flux of O^+ over the nightside of Venus, *Icarus*, *112*(2), 396–404, doi:10.1006/icar.1994.1194.

Brinton, H. C., H. A. Taylor Jr., H. B. Niemann, H. G. Mayr, A. F. Nagy, T. E. Cravens, and D. F. Strobel (1980), Venus nighttime hydrogen bulge, *Geophys. Res. Lett.*, *7*(11), 865–868, doi:10.1029/GL007i011p00865.

Dobe, Z., A. F. Nagy, and J. L. Fox (1995), A Theoretical study concerning the solar cycle dependence of the nightside ionosphere of Venus, *J. Geophys. Res.*, *100*(A8), 14,507–14,513, doi:10.1029/95JA00331.

Gröller, H., V. I. Shematovich, H. I. M. Lichtenegger, H. Lammer, M. Pfleger, Y. N. Kulikov, W. Macher, U. V. Amerstorfer, and H. K. Biernat (2010), Venus' atomic hot oxygen environment, *J. Geophys. Res.*, *115*, E12017, doi:10.1029/2010JE003697.

Hedin, A. E., H. B. Niemann, W. T. Kasprzak, and A. Seiff (1983), Global empirical model of the Venus thermosphere, *J. Geophys. Res.*, *88*(A1), 73–83, doi:10.1029/JA088iA01p00073.

Herzberg, G. (1950), *Molecular Spectra and Molecular Structure*, vol. I, *Spectra of Diatomic Molecules*, 2nd ed., D. Van Nostrand, New York.

Hodges, R. R., Jr. (2000), Distributions of hot oxygen for Venus and Mars, *J. Geophys. Res.*, *105*(E3), 6971–6981, doi:10.1029/1999JE001138.

Huber, K. P., and G. Herzberg (2011), *Constants of Diatomic Molecules: NIST Chemistry WebBook, NIST Stand. Ref. Database 69*, edited by P. J. Linstrom and W. G. Mallard, Natl. Inst. of Stand. and Technol., Gaithersburg, Md. [Available at http://webbook.nist.gov.]

Ip, W. H. (1988), On a hot oxygen corona of Mars, *Icarus*, *76*(1), 135–145, doi:16/0019-1035(88)90146-7.

Keating, G. M., et al. (1985), Models of Venus neutral upper atmosphere: Structure and composition, *Adv. Space Res.*, *5*(11), 117–171, doi:16/0273-1177(85)90200-5.

Kim, J., A. F. Nagy, J. L. Fox, and T. E. Cravens (1998), Solar cycle variability of hot oxygen atoms at Mars, *J. Geophys. Res.*, *103*(A12), 29,339–29,342, doi:10.1029/98JA02727.

Kliore, A. J., J. G. Luhmann, and M. H. G. Zhang (1991), The effect of the solar cycle on the maintenance of the nightside ionosphere of Venus, *J. Geophys. Res.*, *96*(A7), 11,065–11,071, doi:10.1029/91JA00672.

Knudsen, W. C., K. Spenner, K. L. Miller, and V. Novak (1980), Transport of ionospheric O^+ ions across the Venus terminator and implications, *J. Geophys. Res.*, *85*(A13), 7803–7810, doi:10.1029/JA085iA13p07803.

Knudsen, W. C., A. J. Kliore, and R. C. Whitten (1987), Solar cycle changes in the ionization sources of the nightside Venus ionosphere, *J. Geophys. Res.*, *92*(A12), 13,391–13,398, doi:10.1029/JA092iA12p13391.

Krestyanikova, M. A., and V. I. Shematovich (2005), Stochastic models of hot planetary and satellite coronas: A photochemical source of hot oxygen in the upper atmosphere of Mars, *Sol. Syst. Res.*, *39*(1), 22–32, doi:10.1007/s11208-005-0002-9.

Krestyanikova, M. A., and V. I. Shematovich (2006), Stochastic models of hot planetary and satellite coronas: A hot oxygen corona of Mars, *Sol. Syst. Res.*, *40*(5), 384–392, doi:10.1134/S0038094606050030.

Lammer, H., et al. (2006), Loss of hydrogen and oxygen from the upper atmosphere of Venus, *Planet. Space Sci.*, *54*(13–14), 1445–1456, doi:10.1016/j.pss.2006.04.022.

Lichtenegger, H. I. M., H. Gröller, H. Lammer, Y. N. Kulikov, and V. I. Shematovich (2009), On the elusive hot oxygen corona of Venus, *Geophys. Res. Lett.*, *36*, L10204, doi:10.1029/2009GL037575.

Miller, K. L., W. C. Knudsen, K. Spenner, R. C. Whitten, and V. Novak (1980), Solar zenith angle dependence of ionospheric ion and electron temperatures and density on Venus, *J. Geophys. Res.*, *85*(A13), 7759–7764, doi:10.1029/JA085iA13p07759.

Nagy, A. F., and T. E. Cravens (1988), Hot oxygen atoms in the upper atmospheres of Venus and Mars, *Geophys. Res. Lett.*, *15*(5), 433–435, doi:10.1029/GL015i005p00433.

Nagy, A. F., T. E. Cravens, J.-H. Yee, and A. I. F. Stewart (1981), Hot oxygen atoms in the upper atmosphere of Venus, *Geophys. Res. Lett.*, *8*(6), 629–632, doi:10.1029/GL008i006p00629.

Nahar, S. N. (1999), Electron-ion recombination rate coefficients, photoionization cross sections, and ionization fractions for astrophysically abundant elements. II. Oxygen ions, *Astrophys. J. Suppl. Ser.*, *120*(1), 131–145, doi:10.1086/313173.

Sheehan, C. H., and J.-P. St.-Maurice (2004), Dissociative recombination of N_2^+, O_2^+, and NO^+: Rate coefficients for ground state and vibrationally excited ions, *J. Geophys. Res.*, *109*, A03302, doi:10.1029/2003JA010132.

Spenner, K., W. C. Knudsen, and W. Lotze (1995), Ion Density, temperature, and composition of the venus nightside ionosphere during a period of moderate solar activity: Implications for maintaining the central nightside, *J. Geophys. Res.*, *100*(A8), 14,499–14,506, doi:10.1029/95JA01470.

Stancil, P., D. Schultz, M. Kimura, J. Gu, G. Hirsch, and R. Buenker (1999), Charge transfer in collisions of O^+ with H and H^+ with O, *Astron. Astrophys. Suppl. Ser.*, *140*(2), 10, doi:10.1051/aas:1999419.

Terada, N., S. Machida, and H. Shinagawa (2002), Global hybrid simulation of the Kelvin–Helmholtz instability at the Venus ionopause, *J. Geophys. Res.*, *107*(A12), 1471, doi:10.1029/2001JA009224.

Theis, R. F., and L. H. Brace (1993), Solar cycle variations of electron density and temperature in the Venusian nightside ionosphere, *Geophys. Res. Lett.*, *20*(23), 2719–2722, doi:10.1029/93GL02485.

Valeille, A., M. R. Combi, V. Tenishev, S. W. Bougher, and A. F. Nagy (2010), A study of suprathermal oxygen atoms in Mars upper thermosphere and exosphere over the range of limiting conditions, *Icarus*, *206*(1), 18–27, doi:10.1016/j.icarus.2008.08.018.

Vejby-Christensen, L., D. Kella, H. B. Pedersen, and L. H. Andersen (1998), Dissociative recombination of NO^+, *Phys. Rev. A*, *57*(5), 3627–3634, doi:10.1103/PhysRevA.57.3627.

Woodall, J., M. Agúndez, A. J. Markwick-Kemper, and T. J. Millar (2007), The UMIST database for astrochemistry 2006, *Astron. Astrophys.*, *466*(3), 1197–1204, doi:10.1051/0004-6361:20064981.

Wyttenbach, T., C. G. Beggs, and M. T. Bowers (1991), Radiative lifetime measurements of vibrationally excited states of NO^+ ($X^1\Sigma^+$), *Chem. Phys. Lett.*, *177*(3), 239–246, doi:10.1016/0009-2614(91)85023-P.

Zhang, P., V. Kharchenko, M. J. Jamieson, and A. Dalgarno (2009), Energy relaxation in collisions of hydrogen and deuterium with oxygen atoms, *J. Geophys. Res.*, *114*, A07101, doi:10.1029/2009JA014055.

H. K. Biernat, O. Dutuit, H. Gröller, H. Lammer, and H. I. M. Lichtenegger, Space Research Institute, Austrian Academy of Sciences, Schmiedlstraße 6, A-8042 Graz, Austria. (hannes.groeller@oeaw.ac.at)

Y. N. Kulikov, Polar Geophysical Institute, Russian Academy of Sciences, 15 Khalturina St., 183010 Murmansk, Russia.

M. Pfleger, Institute of Physics, University of Graz, Universitätsplatz 5, A-8010 Graz, Austria.

V. I. Shematovich, Institute of Astronomy, Russian Academy of Sciences, 48 Pyatnitskaya St., 119017 Moscow, Russia.